

Evaluation of the size segregation of elemental carbon (EC) emission in Europe: influence on the simulation of EC long-range transportation

Y. Chen^{1,2}, Y. F. Cheng², S. Nordmann^{2,3}, W. Birmili¹, H.A.C. Denier van der Gon⁴, N. Ma^{1,2}, R. Wolke¹, B. Wehner¹, J. Sun¹, G. Spindler¹, Q. Mu², U. Pöschl², H. Su² and A. Wiedensohler¹

[1] {Leibniz-Institute for Tropospheric Research, Leipzig, Germany}

[2] {Multiphase Chemistry Department, Max Planck Institute for Chemistry, Mainz, Germany}

[3] {German Environment Agency, Dessau-Roßlau, Germany}

[4] {TNO, dept. Climate, Air, and sustainability, Utrecht, Netherlands}

Correspondence to: Y. F. Cheng (yafang.cheng@mpic.de) and A. Wiedensohler (ali@tropos.de)

Abstract

Elemental Carbon (EC) has significant impact on human health and climate change. In order to evaluate the size segregation of EC emission in the EUCAARI inventory and investigate its influence on the simulation of EC long-range transportation in Europe, we used the fully coupled online Weather Research and Forecasting/Chemistry model (WRF-Chem) at a resolution of 2 km focusing on a region in Germany, in conjunction with a high-resolution EC emission inventory. The ground meteorology conditions, vertical structure and wind pattern were well reproduced by the model. The simulations of particle number/mass size distributions were evaluated with observations at the central European background site Melpitz. The fine mode particle concentration was reasonably well simulated, but the coarse mode was substantially overestimated by the model mainly due to the plume with high EC concentration in coarse mode emitted by a nearby point source. The comparisons between simulated EC and Multi-angle Absorption Photometers (MAAP) measurements at Melpitz, Leipzig-TROPOS and Bösel indicated that the coarse mode EC (EC_c) emitted from the nearby point sources might be overestimated by a factor of 2-10. The fraction of EC_c was overestimated in the emission inventory by about 10-30% for Russia and 5-10% for Eastern Europe (e.g., Poland and Belarus), respectively. This incorrect size-dependent EC emission

- 1 results in a shorter atmospheric life time of EC particles and inhibits the long range transport
- 2 of EC. A case study showed that this effect caused an underestimation of 20-40% in the EC
- 3 mass concentration in Germany under eastern wind pattern.

1 **1. Introduction**

2 Elemental carbon (EC) and black carbon (BC) are characterized by their strongly radiation
3 absorbing effect (Hansen et al., 2000; Jacobson et al., 2000; Bond et al., 2013) and adverse
4 health effects (Pope et al., 2009; Bond et al., 2013). For climate change, EC is the second
5 strongest contributor to current global warming with a total radiative forcing of about +1.1 W
6 m⁻², just after the carbon dioxide (Bond et al., 2007; Ramanathan et al., 2008). Globally,
7 biomass burning (40%), fossil fuel combustion (40%) and biofuels combustion (20%) are the
8 major source of EC emission (Ramanathan et al., 2008). The EC particles freshly emitted
9 from incomplete combustion have sizes around 100 nm (Rose et al., 2006). The EC particles
10 size segregation information is also very significant for climate, long range transport and
11 health effect. These fine mode (sub-micron) EC particles are much more important than the
12 coarse mode, since fine particles have longer lifetime than coarse particles (Petzold et al.,
13 2012; Croft et al., 2014). They have higher chances to accumulate in the atmosphere and
14 participate long range transportation (e.g. Himalayan and arctic region), furthermore
15 contribute to the global scale climate forcing. Previous studies showed that EC long range
16 transport and deposition on ice could contribute to the glacier melting in Himalayan (Ming et
17 al., 2008) and arctic region (McConnell et al., 2007; Ramanathan et al., 2008). The EC
18 deposition on snow and ice could change the surface albedo, absorbs solar radiation and
19 causes positive climate forcing. Furthermore, for health effect, fine EC particles could
20 translocate from lung to blood with the adsorbed toxic matters (e.g.: heavy metal) inducing
21 many disease (Pope et al., 2009; Meister et al., 2012). The definitions of EC and BC depend
22 on how these species were measured. BC is used for an optical determination and EC for a
23 thermographic measurement method (Nordmann et. al., 2013; Vignati et. al., 2010). However,
24 the discrepancies between EC and BC are usually disregarded, and they are interchangeable in
25 the modelling studies (Vignati et. al., 2010). Nordmann et. al. (2013) showed that the EC and
26 BC were good correlated in the German Ultrafine Aerosol Network (GUAN) sites
27 measurements. Nordmann et. al. (2013) and Nordmann et. al. (2014) indicated that EC in the
28 model can be used as the best approximation of BC in modelling study.

29 The emission inventory is one of the key factors for the evaluation of the EC climate effect
30 with model (Vignati et. al., 2010). The IPCC (IPCC, 2013) reported BC radiative forcing of
31 0.4 (0.05-0.8) W m⁻², 0.2 W m⁻² and 0.04 (0.02-0.09) W m⁻² from fossil fuel combustion,
32 biomass burning and deposition on snow, respectively. The uncertainties in the evaluation of
33 BC global and regional climate effect may be due to uncertainties in BC mass concentrations,

1 which are derived from BC emission and removal processes (Koch et al., 2009). Emissions of
2 carbonaceous aerosols are notoriously uncertain (Denier et al., 2015). The European
3 Environment Agency report (EEA, 2013) indicated that it was almost impossible to evaluate
4 uncertainty overall at the EU level. The uncertainty for EC emissions is at least 50% on global
5 scales, and a factor of 2 to 5 on regional scale (Ramanathan et al., 2008). The uncertainty is
6 originated not only from an instrument measurement uncertainty but also the conditions under
7 which the emission factor measurements take place (Denier et al., 2015). Global emission
8 inventories of EC have been published (e.g.: Bond et. al., 2004; Lamarque et. al., 2010),
9 without size segregation information. An emission inventory for UNECE-Europe of EC
10 (EUCAARI 42-Pan-European Carbonaceous aerosol inventory) has been published with a
11 $1/8^\circ \times 1/16^\circ$ high resolution and separated size mode (PM₁, PM_{1-2.5} and PM_{2.5-10})
12 (Visschedijk et. al., 2008). UNECE-Europe includes the EU27 countries and Albania,
13 Armenia, Azerbaijan, Belarus, Bosnia Herzegovina, Croatia, Georgia, Moldova, Macedonia,
14 Norway, Russia Federation, Serbia and Montenegro, Switzerland, Turkey and Ukraine
15 (Denier et. al., 2015). The EUCAARI inventory consists of anthropogenic emissions by
16 country for the ten Source Nomenclature for Air Pollution (SNAP) sectors: energy
17 transformation, small combustion sources, industrial combustion, industrial processes,
18 extraction of fossil fuels, solvent and product use, road transport, non-road transport, waste
19 handling, and agriculture (Visschedijk et. al., 2008).

20 Lots of modelling studies have been done to evaluate the EC emission and model
21 performance in Europe. Koch et al. (2009) evaluated 17 global models and find out 13 of 17
22 models over-estimate EC in Europe. Stern et al. (2008) compared 5 models result with
23 northern Germany observations, and none of the models could reproduce the high EC
24 concentration at central Europe background station Melpitz. Genberg et al. (2013) pointed out
25 that the EMEP MSC-W model underestimates the EC concentration at Melpitz may because
26 the low model resolution can not represent local effects (like point source). Nordmann et al.
27 (2014) pointed out that the EUCAARI inventory may underestimate the Eastern European EC
28 emission by a factor of about 2, but not considering the size segregation uncertainty of EC
29 emission and its influence on transportation.

30 In this work, a high resolution WRF-Chem simulation was set up conjunction with the
31 EUCAARI EC inventory, focusing on central Europe region. The modelling result was
32 evaluated by the aerosol and EC/BC in-situ measurements from GUAN and HOPE-Melpitz

1 Campaign. The EC emission fraction for coarse (PM_{2.5-10}) mode of the EUCAARI
2 inventory was evaluated. A case study of the high polluted episode in 2009 April (Nordmann
3 et al., 2014) was re-simulated for validating the influence of size segregation in EC
4 transportation.

5 **2. Data & Method**

6 The fully coupled “online” Weather Research and Forecasting/Chemistry model (WRF-Chem
7 V3.5.1) is a state-of-the-art regional air quality model (Grell et al., 2005). It is suitable for a
8 broad spectrum of atmospheric research with horizontal extents ranging from hundreds meters
9 to thousands kilometers. Trace gases, aerosols, and interactive processes with meteorology are
10 simulated with several treatments in the model (Grell et al., 2005). The following is a brief
11 summary of the primary WRF-Chem modules relevant to the current study.

12 In this study, the Carbon-Bond Mechanism version Z (CBMZ, Zaveri et al., 1999; Fast et al.,
13 2006) was used for gas-phase atmospheric chemistry. 67 prognostic species and 164 reactions
14 are included in CBMZ mechanism with a lumped structure approach, which classifies organic
15 compounds according to their internal bond types. Fast-J scheme (Wild et al., 2000; Barnard
16 et al., 2004) was used for calculating the rates for photolytic reactions within CBMZ.

17 The sectional approach MOdel for Simulating Aerosol Interactions and Chemistry (MOSAIC,
18 Zaveri et al., 2008) was applied to better represent the size segregated aerosol properties. In
19 MOSAIC, dry aerosol particles with eight discrete size bins were selected with upper and
20 lower bin diameters defined as shown in Table 1; and particles are assumed to be inter-mixed
21 in each bin (Zaveri et al., 2008). MOSAIC treats the following chemical species: sulfate,
22 methane sulfonate, nitrate, chloride, carbonate, ammonium, sodium, calcium, elemental
23 carbon (EC), organic carbon (OC) and other inorganic mass. Both particle mass and particle
24 number are simulated for each bin. Water uptake or loss will not transfer particles between
25 bins, since bins are based on dry particle diameters (Zaveri et al., 2008). However, particle
26 growth or reduction due to chemical processes (e.g., uptake or release of trace gases, etc.) and
27 physical processes (e.g., coagulation, etc.) will transfer particles between bins (Chapman et al.,
28 2009). In addition, particle coagulation and nucleation processes of sulfuric acid and water
29 vapor are included (Fast et al., 2006; Zaveri et al., 2008). But the formation mechanism of
30 Secondary Organic Aerosol (SOA) is not included in this version (Zaveri et al., 2008).

1 In WRF-Chem, dry (Binkowski et al., 1995) and wet (Easter et al., 2004) deposition processes
2 of aerosol particles are considered. The dry deposition of aerosol in the lowest model layer is
3 derived from the deposition velocities, which is depended on the sublayer resistance,
4 aerodynamic resistance and surface resistance (Grell et al., 2005). The scavenging of cloud-
5 phase and below-cloud aerosol by interception and impaction processes is calculated by look-
6 up tables. It is worth to mention that the particles are treated internally mixed in each bin;
7 therefore the hygroscopicity of EC contained particles tends to be slightly overestimated in
8 the model. Furthermore, the model tends to overestimate the removal rate of EC, especially
9 for the wet deposition processes (Nordmann et al., 2014). In additional, Saide et al. (2012)
10 pointed out that the irreversible removal of aerosol by rain in WRF-Chem might make the wet
11 deposition overestimated. However, it was mostly dominated by dry condition before 16th Sep.
12 2013 in this simulation.

13 As shown in Fig. 1, the simulation consists of 4 nested domains with 39 vertical layers. The
14 spatial resolutions of domains (D01-D04) are 54 km, 18 km, 6 km, and 2 km respectively.
15 The outer domain (D01) covers Europe and the inner domain (D04) focus on Saxony in
16 Germany centered at Melpitz (12.93°E, 51.53°N). The time period from 10th to 20th Sep. 2013
17 was simulated, with 2 days spin-up. The model meteorology fields were driven and forced by
18 Final Analysis (FNL) Operational Global Analysis data (<http://rda.ucar.edu/datasets/ds083.2/>)
19 and sea surface temperature (SST) dataset (<http://polar.ncep.noaa.gov/sst/oper/Welcome.html>)
20 from NCEP (National Center for Environmental Prediction), with 1 degree spatial and 6 hours
21 temporal resolution. The chemical initial and boundary conditions were driven and forced by
22 MOZART-4 global model results (<http://www.acd.ucar.edu/wrf-chem/mozart.shtml>) with 1.9°
23 × 2.5° spatial and 6 hours temporal resolution. The physical and chemical schemes used for
24 the simulation are summarized in Table 2. The aerosol-cloud-radiation interaction is turned on.

25 **2.2 Emissions**

26 The anthropogenic emissions were taken from the Pan-European Carbonaceous aerosol
27 inventory (Visschedijk et al., 2008) for EC and OC, which was developed in the framework of
28 the European Integrated project on Aerosol Cloud Climate and Air Quality interactions
29 (EUCAARI, Kulmala et al., 2011) for the year 2005. It is available on a spatial resolution of
30 1/8° × 1/16° longitude–latitude grid, corresponding to around 7 km (Fig. 1). The EC emissions
31 in different size modes (PM1, PM1-2.5 and PM2.5-10) are provided; more details about the
32 emissions in each mode and the gridding method were given in Denier et al. (2010). The
33 emissions are assumed to be equally distributed over the whole year in this study. A diurnal

1 cycle of the emissions was applied with two maxima, around 07:00 and 18:00 local time. The
2 emissions were allocated in the first 6 layers (from surface to about 550 meters) of the model
3 depending on the emission types, such as area emission, small and large point sources.
4 Nordmann et al. (2014) reported that the EC emission of EUCAARI inventory are around 30%
5 higher than the Lamarque inventory (Bond et al., 2007; Junker et al., 2008; Lamarque et al.,
6 2010) in eastern European countries (Poland, Czech Republic and Belarus).

7 The EMEP inventory for 2013 (<http://www.ceip.at>, Mareckova et. al., 2013), with $0.5^\circ \times 0.5^\circ$
8 spatial resolution, was applied in the model for the other anthropogenic emissions, such as
9 PM, SO₂, NO_x, CO, NH₃, NH₄ and volatile organic compounds (VOC). The emissions of
10 VOCs from EMEP were allocated to compounds used in CBMZ chemical mechanism of
11 WRF-Chem.

12 In this study, biogenic emissions are taken from the Model of Emissions of Gases and
13 Aerosols from Nature (MEGAN, Guenther et al., 2006). The Fire INventory from NCAR
14 (FINN, Wiedinmyer et al., 2011), with 1 km spatial and 1hour temporal resolution, was used
15 in this study. The previous studies reported that the dust emission scheme (Saide et al., 2012)
16 and the sea-salt emission scheme (Saide et al., 2012; Zhang et al., 2013) in WRF-Chem have
17 large uncertainties. However, based on the filter measurements with high volume sampler
18 DIGITEL DHA-80 (Walter Riemer Messtechnik, Germany) at Melpitz, dust and sea-salt
19 contributed less than 3% of aerosol mass in the simulation period. Therefore, the online sea-
20 salt and dust emissions were switched off.

21 **2.3 Observations**

22 The measurements from HOPE-Melpitz Campaign (HD(CP)² Observational Prototype
23 Experiment, <https://icdc.zmaw.de/hopm.html>) and German Ultrafine Aerosol Network
24 (GUAN, Birmili et al., 2009) were used for model evaluation. The meteorological variables
25 (e.g. temperature, relative humidity, wind speed, wind direction), gaseous pollutants (e.g. O₃,
26 NO_x, SO₂) were simultaneously measured. In addition, the radio-sounding data for the
27 stations all-over Europe (<http://www.weather.uwyo.edu/upperair/sounding.html>) were used
28 for evaluating the modelled atmosphere vertical structure.

29 The regional background site Melpitz (12.93°E, 51.53°N) site is representative for a larger
30 rural area in Saxony Germany, detailed description was given in (Brüggenmann et al., 1999;

1 Spindler et al., 2010; Poulain et al., 2011; Spindler et al., 2012). A Twin Differential Mobility
2 Particle Sizer (TDMPS, TROPOS, Leipzig, Germany; Birmili et al., 1999) was used to
3 measure the Particle Number Size Distribution (PNSD) with an electrical mobility diameter
4 between 5 and 800 nm. An Aerodynamic Particle Sizer (APS Model 3320, TSI, Inc.,
5 Shoreview, MN USA) was employed to measure the PNSD with aerodynamic diameter from
6 0.5 to 10 μm . All of them were operated under dry conditions. All the particles were assumed
7 as spherical (shape factor =1), with a density of 1.8 g cm^{-3} for the sub-micrometer particles
8 and 1.5 g cm^{-3} for the super-micrometer particles (Heintzenberg et al., 1998). The mobility
9 diameter can be calculated from the aerodynamic diameter and Particle Mass Size
10 Distribution (PMSD) can be calculated from PNSD, details were described in Heintzenberg et
11 al. (1998). Then PNSD and PMSD in the diameter range of 5-10,000 nm can be derived from
12 TDMPS (5-638 nm) and APS (638-10,000 nm) measurements. A high volume sampler
13 DIGITEL DHA-80 (Walter Rieme Messtechnik, Germany), with sampling flux of about 30
14 m^3h^{-1} , was used for parallel continuous daily samples of PM₁₀, detailed information was
15 given in Spindler et al. (2013). Additionally, radio-sounding measurements were performed in
16 Melpitz on the days 11th-14th, 17th and 19th September 2013.

17 At Melpitz, Bösel (7.94°E, 53.0°N) and Leipzig-TROPOS (12.43°E 51.35°N), Multi-angle
18 Absorption Photometers (MAAP Model 5012, Thermo, Inc., Waltham, MA USA) were
19 employed to determine the particle light absorption coefficient for dry particles. All these
20 stations are defined as rural or urban background station. The MAAPs were measured with 10
21 μm cut-off inlet and the corrected mass absorption cross-section (MAC) of $5 \text{ m}^2\text{g}^{-1}$ was used
22 to derive the BC mass concentration for Melpitz (Genberg et al., 2013), and the manual
23 suggested MAC of $6.6 \text{ m}^2\text{g}^{-1}$ was used for Bösel and Leipzig-TROPOS. Since EC and
24 absorption-related BC were highly correlated in Germany GUAN Network sites (Nordmann
25 et al., 2013), we used the MAAP measured BC as the best approximation of EC (Nordmann et
26 al., 2014) in this study.

27 **3. Result & Discussion**

28 **3.1 Meteorology conditions**

29 The WRF performance on simulating the meteorological fields was evaluated with the
30 Melpitz ground measurements data and radio-sounding measurements over the whole Europe.
31 The wind pattern in simulated time period was dominated by westerly winds in Melpitz (Fig.

1 2d). It was mostly dominated by dry condition between 13th and 15th Sep. in Melpitz. The air
2 mass of northern Germany changed from continental to maritime after 15th Sep. The maritime
3 air mass from North Sea was relatively clean, with less anthropogenic pollutants. In 15-16th
4 Sep., the concentration of primary gaseous pollutant NO was significantly lower at Melpitz
5 than 13-14th Sep. (Fig. S1), and also the PM10, PM2.5 and PM1 mass concentrations were
6 reduced by more than 50%.

7 As shown in Fig. 2, the variances of temperature, relative humidity, wind speed and wind
8 direction were validated with the ground measurements, with a correlation coefficient (R^2) of
9 0.88, 0.72, 0.74, and 0.74 respectively. The peaks in NO concentration can be reproduced by
10 the model, although overestimated in the peaks (Fig. S1). The transport process and emission
11 location were also supposed to be well described in the model, because NO has very short
12 lifetime and therefore a good indicator of nearby sources. These results show that the WRF
13 model can well reproduce the near surface meteorological condition and transport processes at
14 Melpitz.

15 The vertical gradient of the potential temperature is an important indicator for the stability of
16 atmosphere. Fig. S2 shows a R^2 map of comparison between radio-sounding observed and
17 simulated vertical potential temperature in planetary boundary layer (PBL, under 3 km). The
18 R^2 values were higher than 0.8 for all the stations over Europe, especially for Melpitz region
19 the R^2 was higher than 0.9. The comparison at the Melpitz site is shown in Table 3, together
20 with some profile examples in Fig. S3. The meteorological vertical structure was well
21 captured by the model, with R^2 value of 0.98, 0.84, 0.93 and 0.70 for the potential temperature,
22 water vapor mixing ratio, wind speed and wind direction respectively. The results indicate
23 that WRF well simulated the meteorological vertical structure and wind pattern, especially in
24 central Europe (Melpitz region with 2 km resolution).

25 **3.2 Particle size distribution**

26 The modelled particle number size distribution (PNSD) and particle mass size distribution
27 (PMSD) for Melpitz were compared with the measurements, shown in Fig. 3. For the fine
28 mode (PM1, or sub-micron particles) aerosol the agreement is acceptable, but the model
29 significantly overestimated the coarse mode (PM2.5-10) mass/number. The meteorology
30 condition was well reproduced by the model. The transportation process was also supposed to

1 be well simulated. It indicates that there may be some unrealistic sources of particles larger
2 than 2.5 μm included in the model, which leads to the overestimation of coarse mode. The
3 detailed discussion about the unrealistic sources will be given in section 3.3.

4 We found out that EC had a very high contribution of modelled coarse mode aerosol mass
5 when the EC plumes hit Melpitz (Fig. 4a and Fig. 5a). In order to investigate the reasons of
6 the EC plumes and its influence on coarse mode overestimation, a more detailed case study
7 for the plume episode in the morning of 13th September will be given in section 3.3.

8 **3.3 Elemental carbon point source size segregation and evaluation**

9 In order to evaluate the EC emission in central Europe and investigate local effect of point
10 source, MAAP measurements of 3 background sites (Melpitz, Leipzig-TROPOS and Bösel)
11 were compared with modelled results (Fig. 4). In Leipzig-TROPOS, the relatively high EC
12 concentration in the morning and night but low concentration at the noontime could be
13 resulted from the development of planet boundary layer and traffic rush hours. According to
14 modelled transportations, Melpitz and Bösel were influenced by the point source plume, but
15 Leipzig-TROPOS was not (see Fig. 5b and Fig. S4). Here we use MAAP instead of DIGITEL
16 measurement to compare with the model output, because only MAAP data are available for
17 all those three sites and the higher temporal resolution of the MAAP is better for investigating
18 the point source plume influence.

19 The model substantially overestimated the EC concentration in Melpitz especially for high
20 episode peaks (Fig. 4a), during which the modelled EC concentration in PM10 can reach up to
21 about 3-4 times higher than that in PM2.5. While outside the peaks, EC concentration in
22 PM10 and PM2.5 were very close to each other. Comparing with MAAP measurement, EC in
23 PM10 was on average overestimated by a factor of 2.8 at Melpitz, and by a factor up to 6-10
24 for the peak periods. This overestimation of EC was due to the plume from a point source
25 emission of type SNAP-5 (extraction and distribution fossil fuels, nomenclature described in
26 Visschedijk et al., 2008 and Pouliot et al., 2012) located between Leipzig and Melpitz. Fig. 5
27 is an example snapshot showing the EC plume passing through Melpitz at 05:00 a.m. on 13th
28 Sep. 2013. Plumes from the same sources also similarly influenced other peak periods to
29 different extend. When the plume hitting Melpitz, the overestimation of EC concentration was
30 substantial even when the uncertainties in the modelled transportation within 12*12 km² was
31 accounted for (shaded area in Fig. 4a), and EC contributed 30-67% of coarse mode aerosol

1 mass. At the same time, Leipzig was not influenced by point source plume, because of the
2 prevailing westerly wind in domain D04 (Fig. 5b). The comparison at the Leipzig-TROPOS
3 site was thus much better (Fig. 4b). There, EC was only slightly overestimated by less than
4 40%, which may be due to the seasonal variability and/or reducing emissions (~25% from
5 2010 to 2013, based on long term MAAP measurements in Leipzig-TROPOS and DIGITEL
6 measurements in Melpitz) in context of Saxony “low emission zone” policy since March 2011
7 (http://gis.uba.de/website/umweltzonen/umweltzonen_en.php). The different behaviors of
8 model at these two sites indicate that the coarse mode EC emission in the point sources near
9 Melpitz can be significantly overestimated.

10 This EC plume effect was not only found in Melpitz. As shown in Fig. S4, Bösel was also
11 influenced by a nearby EC point source in the morning of 13th and 14th Sep. 2013 (also Fig.
12 4c). The EC concentration was overestimated and had a high coarse mode fraction, similar to
13 Melpitz. However, the overestimation of EC was not as significant as for Melpitz, with ~87%
14 on average and about 200-400% during the peak periods. The fraction of EC in coarse mode
15 was also not as high as in Melpitz. One reason could be the lower intensity of the point source
16 nearby Bösel than the one near Melpitz (Fig. S4). Another reason may be the artificial dilution
17 of local emissions by the coarser modelling resolution (Genberg et al., 2013), because we only
18 have the highest resolution of 2 km covering the regions around Melpitz (D04), but 6 km
19 resolution for Bösel (D03).

20 These results imply that the EC point sources in Germany can be overestimated by a factor of
21 2-10 in the EUCAARI emission inventory, especially for the coarse mode EC emission in the
22 large point sources. To further evaluate the coarse mode EC emission (EC_c, EC in PM_{2.5-10})
23 over the whole Europe, we first checked the emission fraction of EC_c to the total EC in
24 EUCAARI inventory. As shown in Fig. 6a, this fraction is generally lower than 10% over
25 large regions in Western Europe. For almost all of the point sources, the EC_c emission
26 fractions are higher than 30% (Fig. 6b), within which there are 3 and 10 point sources
27 surrounding Melpitz and Bösel region, respectively, with EC_c emission fractions even higher
28 than 80% (Table S1 and Fig. 6b). It is worth to mention that these point sources with high
29 EC_c emission fractions also have a very high total EC emission rate. For example, the point
30 source, influencing Melpitz in the morning of 13th Sep, is the largest point source for SNAP-5
31 in Germany with a share of about 20% in the total EC point emission. EC emissions from the
32 SNAP-5 point sources are originated from coal-mining, storage and handling (Visschedijk et

1 al., 2008; Pouliot et al., 2012; Denier et al., 2015), for which a relatively high fraction in
2 coarse mode emission is expected. Therefore, the emission fraction of EC_c may be true. But,
3 the total EC emission rate might be too high due to the overestimation of EC scaling factor
4 out of all emitted compounds. But it is hard to quantify it due to the fact that little data are
5 available for the storage and handling of coal, and about chemical composition and size
6 distribution of the emission in SNAP-5 type of emissions.

7 Note that the dry and wet deposition processes also contribute to the uncertainty of the
8 modeling results. The dominant removal process for EC is wet deposition (Genberg et al.,
9 2013); Croft et al. (2005) estimated that about 75% of the EC is removed by wet deposition
10 and 25% by dry deposition, based on global model runs. And the wet deposition of EC may
11 be overestimated in the WRF-Chem model due to the irreversible removal process (Yang et
12 al., 2011; Saide et al., 2012) and the internal mixture of EC (Nordmann et al., 2014). It
13 indicates that the overestimation of EC should be resulted from the emission source instead of
14 deposition process, although the uncertainty of deposition would influence the emission
15 evaluation results. More measurements and modeling studies are still needed for the
16 quantified evaluate the deposition processes uncertainty.

17 **3.4 Influence on elemental carbon transportation**

18 EC is in general mostly emitted in the fine mode, especially for the area emissions (Echalar et
19 al., 1998; Hitzenberger et al., 2001; Kuenen et al., 2014), although the SNAP-5 point sources
20 may be an exception. The major SNAP-5 point sources giving coarse EC are coal mines and
21 originate from storage and handling – dust being released due to loading & unloading, driving
22 on the premises etc. Based on the EUCAARI inventory, the average EC_c emission fraction for
23 Western Europe is around 5%, also about 5% in Germany of year 2009 TNO-MACC_II
24 inventory (Kuenen et. al., 2014). This is consistent with previous knowledge. But on the
25 contrast to the generally low EC_c emission fraction, this fraction is relatively high in Eastern
26 Europe (e.g. Poland, Slovakia and Belarus) of about 15-20%, and about 35% in Poland of
27 TNO-MACC_II inventory (Kuenen et. al., 2014). For Russia (including Kaliningrad in the
28 north of Poland) and Moldova the fraction can reach up to 20-40%, and about 17% in Russia
29 of TNO-MACC_II inventory (Kuenen et. al., 2014). As shown in the long-term (2003-2011)
30 filter measurement study at Melpitz (Spindler et al., 2013), in the eastern wind dominated
31 period when the air mass came from Eastern Europe and Russia, the EC coarse mode mass
32 fraction was only in the range of 4-15% (~10% in average). Assuming that EC particles

1 would not change the size during transportation, EUCAARI inventory may overestimate the
2 fraction of ECc about 5-10% for Eastern Europe and 10-30% for Russia.

3 The life-time for fine mode particles is about 5-7 days, but only 1-2 days for the coarse mode
4 aerosol (Jaenicke et al., 1980; Petzold et al., 2012; Croft et al., 2014). Therefore, the fine
5 mode EC particles have more time to accumulate in the atmosphere. To evaluate the influence
6 of this high coarse mode EC emission fraction in Eastern Europe on EC's long-range
7 transportation, we constructed the following concept model. In a steady state, where sources
8 are continuous and there is a quasi-equilibrium between sources and sinks such that the EC
9 concentration is constant in time. For the same emission rate of EC, the equilibrium mass
10 concentration of fine mode will be 2-3 times higher than coarse mode as described in Eq. (1)
11 (Croft et al., 2014).

$$12 \quad \frac{dC(t)}{dt} = S(t) - \frac{C(t)}{\tau(t)} \quad (1)$$

13 where $C(t)$ is the EC concentration at time t , $S(t)$ is the source rate, and $\tau(t)$ is the removal
14 timescale. In the steady state, a quasi-equilibrium between sources and sinks, $\tau(t)$ is defined as
15 lifetime (Croft et al., 2014). Then the deposition rate (sink rate), with unit of percentage per
16 second, is proportional to $1/\tau(t)$ for stationary concentrations. The deposition rate of EC in
17 coarse mode is 2-3 times higher than in fine mode.

18 On the other hand, longer lifetime makes fine mode EC particles have more opportunity to be
19 transported from Eastern Europe to Melpitz. In the following scenario, the particles were
20 emitted instantly into the air mass, which was assumed to be transported by an eastern wind
21 pattern with 5 m s^{-1} speed. It will take about 4-5 days from Moskva to Melpitz, and 1-2 days
22 from Warsaw Poland. During the transport, only the deposition process was active, without
23 subsequent emission. About 30-55% and 65-85% of fine mode EC can be transported to
24 Melpitz from Moskva and Warsaw Poland respectively, but just 5-20% and 10-60% for the
25 coarse mode EC can make the same way (Fig. 7).

26 The overestimation of ECc emission fraction in EUCAARI inventory made less EC
27 transported from the Eastern Europe and Russia to Melpitz. This may be one reason of the
28 underestimation of the EC mass concentration in the other studies under eastern wind pattern.

1 For instance, Genberg et al. (2013) and Nordmann et al. (2014) reported an underestimation
2 of EC in Europe with the simulation of EUCAARI inventory.

3 Nordmann et al. (2014) reported an underestimation about 50% of EC mass concentration in
4 Germany during March-April 2009, especially for the period when air mass approached the
5 observation sites from eastern directions. And they suspected that the EC emission in Eastern
6 Europe may be underestimated by a factor of 2 to 5. In order to investigate the possible
7 influence of the overestimated ECc emission fraction in Eastern Europe in this case, we re-
8 simulated the same time period as in Nordmann et al. (2014) with the adjusted EC emission
9 inventory. The ECc emission fraction was adjusted to 5% (the average value for Western
10 Europe, longitude<15°E) if it is higher than 5% in Eastern Europe (longitude>15°E). The new
11 simulation and the results of Nordmann et al. (2014) are shown in Table 4. The air mass back
12 trajectories of the high EC concentration period (2009.04.04, Nordmann et al., 2014) is shown
13 in Fig. 6a. The back trajectories were calculated based on the GDAS (with 0.5° resolution)
14 dataset with the Hysplit model (http://www.arl.noaa.gov/HYSPLIT_info.php). The
15 underestimation for EC was significantly improved at B ösel and Leipzig-TROPOS. For B ösel,
16 the mean normalized bias (MNB) increased from -21% to 13% and R² from 0.61 to 0.81; for
17 Leipzig-TROPOS, the MNB increased from -70% to -47% and R² from 0.35 to 0.69. The
18 results of Hohenpei ßenberg and Zugspitze were not significantly changed, with less than 10%
19 differences in MNB. This is because the air masses of B ösel and Leipzig-TROPOS originated
20 from Eastern Europe passing through Poland, where the ECc emission fraction in EUCAARI
21 inventory is high. But it was not the case for Southeast Europe, where the air masses of
22 Hohenpei ßenberg and Zugspitze originated from (Fig. 6a). Thus, it indicate that the
23 Nordmann et al. (2014)'s conclusion of underestimation of EC emission in Eastern Europe
24 for 2009 is generally correct, especially for Southeastern Europe (e.g.: Austria, Slovenia,
25 Croatia etc.). However, the overestimation of ECc emission fraction in Eastern Europe (e.g.:
26 Poland, Belarus, Russia etc.) could be another reason for the underestimation of modeled EC
27 mass concentration in the eastern wind pattern. It contributed about 20-40% underestimation
28 of the EC mass concentration in Germany. This is consistent with the result of concept model,
29 which showed the adjustment of ECc emission fraction in Warsaw Poland would make about
30 25-55% difference of EC transported to Melpitz.

31 **4 Conclusions**

1 A WRF-Chem simulation was performed for the period between 10th and 20th Sep. 2013, with
2 an inner most domain of 2 km resolution for the Melpitz region in eastern Germany. The high
3 resolution EUCAARI inventory of EC emission was applied in the model. The measurements
4 of HOPE-Melpitz Campaign and GUAN network project were used for modelling results
5 validation.

6 The comparison of particle number/mass size distributions showed that the coarse mode
7 particle concentration was substantially overestimated by the model. However, the
8 meteorology and transport process were well simulated, because of the good agreement with
9 the ground-based and radio-sounding meteorological measurements. These results indicated
10 that the overestimation of the coarse mode particle should mostly come from the uncertainty
11 of emission inventories. The comparisons of EC mass concentrations in Melpitz, Leipzig-
12 TROPOS and Bösel indicated that the EC point sources may be overestimated by a factor of
13 2-10, which made a remarkable unrealistic plume in Melpitz.

14 The coarse mode EC emission fraction was substantially overestimated in Eastern Europe
15 (e.g.: Poland, Belarus etc.) and Russia by EUCAARI inventory, with about 10-30% for Russia
16 and 5-10% for the Eastern Europe countries. A concept model and a case study were designed
17 to interpret the influence of this overestimation on EC long range transportation. Due to the
18 overestimation of ECc emission fraction, EC mass transported from Moskva to Melpitz would
19 decrease about 25-35% of ECc mass concentration, and decrease about 25-55% from Warsaw
20 to Melpitz. This is because the coarse mode particle has a shorter life-time and therefore less
21 opportunity for being long range transported and accumulated in the atmosphere. The Mar.-
22 Apr. 2009 case (Nordmann et al., 2014) was re-simulated with adjusted ECc emission fraction
23 in Eastern Europe in order to validate the influence on transportation. The result showed that
24 the overestimation of ECc emission fraction in Eastern Europe was one reason of the
25 underestimation of EC in Germany, when the air masses came from eastern direction. It
26 contributed to an underestimation of about 20-40%.

27 Will the health and climatic effects of atmospheric EC particles be local, regional or global?
28 This is some extent determined by the transportation of EC, which is largely influenced by its
29 size distribution. The size segregation information of EC particles should be carefully
30 considered in the model validation and climate change evaluation studies. Unfortunately, the
31 size segregation information is not included in most of the current global EC emission

1 inventories, and the size segregation in EUCAARI inventory only covers Europe and is still
2 with high uncertainty. More EC particle size distribution measurements (e.g.: online analysis
3 of SP2, offline analysis of Berner / MOUDI samples, etc.) and long term model simulation
4 studies are needed to further improve the EC emission inventories.

5 **Acknowledgements:** Continuous aerosol measurements at Melpitz were supported by the
6 German Federal Environment Ministry (BMU) grants F&E 370343200 (German title:
7 “Erfassung der Zahl feiner und ultrafeiner Partikel in der Außenluft”) and F&E 371143232
8 (German title: “Trendanalysen gesundheitsgefährdender Fein- und Ultrafeinstaubfraktionen
9 unter Nutzung der im German Ultrafine Aerosol Network (GUAN) ermittelten
10 Immissionsdaten durch Fortführung und Interpretation der Messreihen”). The HOPE
11 campaign was funded by the German Research Ministry under the project number 01LK1212
12 C. The work of Y. F. Cheng and H. Su was supported by the Max Planck Society (MPG) and
13 National Natural Science Foundation of China (41330635). We would also like to thank
14 Markus Hermann and Sascha Pfeifer for useful suggestions.

15

1 **References:** Barnard, J. C., Chapman, E. G., Fast, J. D., Schemlzer, J. R., Slusser, J. R., and
2 Shetter, R. E.: An evaluation of the FAST-J Photolysis Algorithm for predicting nitrogen
3 dioxide photolysis rates under clear and cloudy sky conditions, *Atmos. Environ.*, 38, 3393–
4 3403, 2004. Binkowski, F. S. and Shankar, U.: The Regional Particulate Matter Model: 1.
5 Model description and preliminary results, *J. Geophys. Res.*, 100, 26191–26209,
6 doi:10.1029/95JD02093, 1995.

7 Birmili, W., Stratmann, F., and Wiedensohler, A.: Design of a DMAbased size spectrometer
8 for a large particle size range and stable operation, *J. Aerosol Sci.*, 30, 549–533, 1999.

9 Birmili, W., Weinhold, K., Nordmann, S., Wiedensohler, A., Spindler, G., Müller K.,
10 Herrmann, H., Gnauk, T., Pitz, M., Cyrus, J., Flentje, H., Nickel, C., Kuhlbusch, T., Löschau
11 G., Haase, D., Meinhardt, F., Schwerin, A., Ries, L., and Wirtz, K.: Atmospheric aerosol
12 measurements in the German Ultrafine Aerosol Network (GUAN) – Part – soot and particle
13 number size distributions, *Gefährst. Reinhalt. L.*, 69, 137–145, 2009.

14 Bond, T. C., Streets, D. G., Yarber, K. F., Nelson, S. M., Woo, J., and Klimont, Z.: A
15 technologybased global inventory of black and organic carbon emissions from combustion, *J.*
16 *Geophys. Res.*, 109, D14203, doi:10.1029/2003JD003697, 2004.

17 Bond, T. C., Bhardwaj, E., Dong, R., Jogani, R., Jung, S., Roden, C., Streets, D. G., and
18 Trautmann, N. M.: Historical emissions of black and organic carbon aerosol from energy-
19 related combustion, 1850–2000, *Global Biogeochem. Cy.*, 21, GB2018,
20 doi:10.1029/2006GB002840, 2007.

21 Bond, T. C., Doherty, S. J., Fahey, D. W., Forster, P. M., Berntsen, T., DeAngelo, B. J.,
22 Flanner, M. G., Ghan, S., Kärcher, B., Koch, D., Kinne, S., Kondo, Y., Quinn, P. K., Sarofim,
23 M. C., Schultz, M. G., Schulz, M., Venkataraman, C., Zhang, H., Zhang, S., Bellouin, N.,
24 Guttikunda, S. K., Hopke, P. K., Jacobson, M. Z., Kaiser, J. W., Klimont, Z., Lohmann, U.,
25 Schwarz, J. P., Shindell, D., Storelvmo, T., Warren, S. G., and Zender, C. S.: Bounding the
26 role of black carbon in the climate system: a scientific assessment, *J. Geophys. Res.-Atmos.*,
27 118, 5380– 5552, doi:10.1002/jgrd.50171, 2013.

28 Brüggemann E. and Spindler, G.: Wet and dry deposition of sulphur at the site Melpitz in East
29 Germany, *Water Air Soil Poll.*, 109, 81–99, 1999.

30 Chapman, E. G., Gustafson Jr., W. I., Easter, R. C., Barnard, J. C., Ghan, S. J., Pekour, M. S.,
31 and Fast, J. D.: Coupling aerosol-cloud-radiative processes in the WRF-Chem model:
32 Investigating the radiative impact of elevated point sources, *Atmos. Chem. Phys.*, 9, 945–964,

1 doi:10.5194/acp-9-945-2009, 2009.

2 Croft, B., Pierce, J. R., and Martin, R. V.: Interpreting aerosol lifetimes using the GEOS-
3 Chem model and constraints from radionuclide measurements, *Atmos. Chem. Phys.*, 14,
4 4313– 4325, doi:10.5194/acp-14-4313-2014, 2014.

5 Denier van der Gon, H. A. C., Visschedijk, A., Van der Brugh, H., and Dröge, R.: A High
6 Resolution European Emission Database for the Year 2005, a Contribution to the UBAproject
7 PAREST: Particle Reduction Strategies, TNO report TNO-034-UT-2010-01895_RPTML,
8 published by the German Federal Environment Agency (Umweltbundesamt) as Texte
9 41/2013, Utrecht, available at: <https://www.umweltbundesamt.de/publikationen>, 2010.

10 Denier van der Gon, H. A. C., Bergström, R., Fountoukis, C., Johansson, C., Pandis, S. N.,
11 Simpson, D., and Visschedijk, A. J. H.: Particulate emissions from residential wood
12 combustion in Europe – revised estimates and an evaluation, *Atmos. Chem. Phys.*, 15, 6503–
13 6519, doi:10.5194/acp-15-6503-2015, 2015.

14 Easter, R. C., Ghan, S. J., Zhang, Y., Saylor, R. D., Chapman, E. G., Laulainen, N. S., Abdul-
15 Razzak, H., Leung, L. R., Bian, X., and Zaveri, R. A.: MIRAGE: model description and
16 evaluation of aerosols and trace gases, *J. Geophys. Res.*, 109, D20210,
17 doi:10.1029/2004JD004571, 2004.

18 Echalar, F., Artaxo, P., Martins, J. V., Yamasoe, M., Gerab, F., Maenhaut, W., and Holben, B.:
19 Long-term monitoring of atmospheric aerosols in the Amazon Basin: source identification and
20 apportionment, *J. Geophys. Res.-Atmos.*, 103, 31849–31864, 1998.

21 EEA: (European Environment Agency): European Union Emission Inventory Report 1990–
22 2011 Under the UNECE Convention on Long-range Transboundary Air Pollution (LRTAP),
23 EEA Technical report No. 10/2013, Copenhagen, doi:10.2800/44480, 2013.

24 Fast, J. D., Gustafson Jr., W. I., Easter, R. C., Zaveri, R. A., Barnard, J. C., Chapman, E. G.,
25 Grell, G. A., and Peckham, S. E.: Evolution of ozone, particulates, and aerosol direct radiative
26 forcing in the vicinity of Houston using a fully coupled meteorology-chemistry-aerosol
27 model, *J. Geophys. Res.*, 111, D21305, doi:10.1029/2005JD006721, 2006.

28 Genberg, J., Denier van der Gon, H. A. C., Simpson, D., Swietlicki, E., Areskou, H.,
29 Beddows, D., Ceburnis, D., Fiebig, M., Hansson, H. C., Harrison, R. M., Jennings, S. G.,
30 Saarikoski, S., Spindler, G., Visschedijk, A. J. H., Wiedensohler, A., Yttri, K. E., and
31 Bergström, R.: Light-absorbing carbon in Europe – measurement and modelling, with a focus
32 on residential wood combustion emissions, *Atmos. Chem. Phys.*, 13, 8719–8738,

1 doi:10.5194/acp-13-8719-2013, 2013.

2 Grell, G. A., Peckham, S. E., Schmitz, R., McKeen, S. A., Frost, G., Skamarock, W. C., and
3 Eder, B.: Fully coupled “online” chemistry within the WRF model, *Atmos. Environ.*, 39,
4 6957–6975, 2005.

5 Guenther, A., Karl, T., Harley, P., Wiedinmyer, C., Palmer, P. I., and Geron, C.: Estimates of
6 global terrestrial isoprene emissions using MEGAN (Model of Emissions of Gases and
7 Aerosols from Nature), *Atmos. Chem. Phys.*, 6, 3181–3210, doi:10.5194/acp-6-3181-2006,
8 2006.

9 Hansen, J. E., Sato, M., Ruedy, R., Lacis, A., and Oinas, V.: Global warming in the twenty-
10 first century: an alternative scenario, *P. Natl. Acad. Sci. USA*, 97, 9875–9880, 2000.

11 Heintzenberg, J., Müller, K., Birmili, W., Spindler, G., and Wiedensohler, A.: Mass-related
12 aerosol properties over the Leipzig Basin, *J. Geophys. Res.-Atmos.*, 103, 13125–13135, 1998.

13 Hitzenberger, R. and Tohno, S.: Comparison of black carbon (BC) aerosols in two urban areas
14 – concentrations and size distributions, *Atmos. Environ.*, 35, 2153–2167, 2001.

15 IPCC A R.: *Climate Change 2013: The Physical Science Basis, Contribution of Working*
16 *Group I to the Fifth Assessment Report of the Intergovernmental Panel on Climate Change,*
17 *Report, Cambridge University Press, New York, 2013.*

18 Jacobson, M. Z.: A physically-based treatment of elemental carbon optics: implications for
19 global direct forcing of aerosols, *Geophys. Res. Lett.*, 27, 217–220,
20 doi:10.1029/1999GL010968, 2000. Jaenicke, R.: Atmospheric aerosols and global climate, *J.*
21 *Aerosol Sci.*, 11, 577–588, 1980.

22 Junker, C. and Liousse, C.: A global emission inventory of carbonaceous aerosol from historic
23 records of fossil fuel and biofuel consumption for the period 1860–1997, *Atmos. Chem.*
24 *Phys.*, 8, 1195–1207, doi:10.5194/acp-8-1195-2008, 2008.

25 Koch, D., Schulz, M., Kinne, S., McNaughton, C., Spackman, J. R., Balkanski, Y., Bauer, S.,
26 Berntsen, T., Bond, T. C., Boucher, O., Chin, M., Clarke, A., De Luca, N., Dentener, F., Diehl,
27 T., Dubovik, O., Easter, R., Fahey, D. W., Feichter, J., Fillmore, D., Freitag, S., Ghan, S.,
28 Ginoux, P., Gong, S., Horowitz, L., Iversen, T., Kirkevåg, A., Klimont, Z., Kondo, Y., Krol,
29 M., Liu, X., Miller, R., Montanaro, V., Moteki, N., Myhre, G., Penner, J. E., Perlwitz, J.,
30 Pitari, G., Reddy, S., Sahu, L., Sakamoto, H., Schuster, G., Schwarz, J. P., Seland, Ø., Stier, P.,
31 Takegawa, N., Takemura, T., Textor, C., van Aardenne, J. A., and Zhao, Y.: Evaluation of

1 black carbon estimations in global aerosol models, *Atmos. Chem. Phys.*, 9, 9001–9026,
2 doi:10.5194/acp-9-9001-2009, 2009.

3 Kuenen, J. J. P., Visschedijk, A. J. H., Jozwicka, M., and Denier van der Gon, H. A. C.: TNO-
4 MACC_II emission inventory; a multi-year (2003–2009) consistent high-resolution European
5 emission inventory for air quality modelling, *Atmos. Chem. Phys.*, 14, 10963–10976,
6 doi:10.5194/acp-14-10963-2014, 2014.

7 Kulmala, M., Asmi, A., Lappalainen, H. K., Baltensperger, U., Brenguier, J.-L., Facchini, M.
8 C., Hansson, H.-C., Hov, Ø., O’Dowd, C. D., Pöschl, U., Wiedensohler, A., Boers, R.,
9 Boucher, O., de Leeuw, G., Denier van der Gon, H. A. C., Feichter, J., Krejci, R., Laj, P.,
10 Lihavainen, H., Lohmann, U., McFiggans, G., Mentel, T., Pilinis, C., Riipinen, I., Schulz, M.,
11 Stohl, A., Swietlicki, E., Vignati, E., Alves, C., Amann, M., Ammann, M., Arabas, S., Artaxo,
12 P., Baars, H., Beddows, D. C. S., Bergström, R., Beukes, J. P., Bilde, M., Burkhardt, J. F.,
13 Canonaco, F., Clegg, S. L., Coe, H., Crumeyrolle, S., D’Anna, B., Decesari, S., Gilardoni, S.,
14 Fischer, M., Fjaeraa, A. M., Fountoukis, C., George, C., Gomes, L., Halloran, P., Hamburger,
15 T., Harrison, R. M., Herrmann, H., Hoffmann, T., Hoose, C., Hu, M., Hyvärinen, A., Hörrak,
16 U., Iinuma, Y., Iversen, T., Josipovic, M., Kanakidou, M., Kiendler-Scharr, A., Kirkevåg, A.,
17 Kiss, G., Klimont, Z., Kolmonen, P., Komppula, M., Kristjánsson, J.-E., Laakso, L.,
18 Laaksonen, A., Labonnote, L., Lanz, V. A., Lehtinen, K. E. J., Rizzo, L. V., Makkonen, R.,
19 Manninen, H. E., McMeeking, G., Merikanto, J., Minikin, A., Mirme, S., Morgan, W. T.,
20 Nemitz, E., O’Donnell, D., Panwar, T. S., Pawlowska, H., Petzold, A., Pienaar, J. J., Pio, C.,
21 Plass-Duelmer, C., Prévôt, A. S. H., Pryor, S., Reddington, C. L., Roberts, G., Rosenfeld, D.,
22 Schwarz, J., Seland, Ø., Sellegri, K., Shen, X. J., Shiraiwa, M., Siebert, H., Sierau, B.,
23 Simpson, D., Sun, J. Y., Topping, D., Tunved, P., Vaattovaara, P., Vakkari, V., Veefkind, J. P.,
24 Visschedijk, A., Vuollekoski, H., Vuolo, R., Wehner, B., Wildt, J., Woodward, S., Worsnop, D.
25 R., van Zadelhoff, G.-J., Zardini, A. A., Zhang, K., van Zyl, P. G., Kerminen, V.-M., S
26 Carslaw, K., and Pandis, S. N.: General overview: European Integrated project on Aerosol
27 Cloud Climate and Air Quality interactions (EUCAARI) – integrating aerosol research from
28 nano to global scales, *Atmos. Chem. Phys.*, 11, 13061–13143, doi:10.5194/acp-11-13061-
29 2011, 2011.

30 Lamarque, J.-F., Bond, T. C., Eyring, V., Granier, C., Heil, A., Klimont, Z., Lee, D., Liousse,
31 C., Mieville, A., Owen, B., Schultz, M. G., Shindell, D., Smith, S. J., Stehfest, E., Van
32 Aardenne, J., Cooper, O. R., Kainuma, M., Mahowald, N., McConnell, J. R., Naik, V., Riahi,
33 K., and van Vuuren, D. P.: Historical (1850–2000) gridded anthropogenic and biomass

1 burning emissions of reactive gases and aerosols: methodology and application, *Atmos.*
2 *Chem. Phys.*, 10, 7017–7039, doi:10.5194/acp-10-7017-2010, 2010.

3 Mareckova, K., Wankmueller, R., Moosmann, L., and Pinterits, M.: Inventory Review 2013:
4 Re- view of Emission Data reported under the LRTAP Convention and NEC Directive, Stage
5 1 and 2 review, Status of Gridded Data and LPS Data, STATUS Report 1/2013,
6 Umweltbundesamt GmbH, Vienna, Austria, 2013.

7 McConnell, J. R., Edwards, R., Kok, G. L., Flanner, M. G., Zender, C. S., Saltzman, E. S.,
8 Banta, J. R., Pasteris, D. R., Carter, M. M., and Kahl, J. D. W.: 20th-century industrial black
9 carbon emissions altered arctic climate forcing, *Science*, 317, 1381–1384, 2007.

10 Meister, K., Johansson, C., and Forsberg, B.: Estimated short-term effects of coarse particles
11 on daily mortality in Stockholm, Sweden, *Environ. Health Persp.*, 120, 431–436, 2012.

12 Ming, J., Cachier, H., Xiao, C., Qin, D., Kang, S., Hou, S., and Xu, J.: Black carbon record
13 based on a shallow Himalayan ice core and its climatic implications, *Atmos. Chem. Phys.*, 8,
14 1343–1352, doi:10.5194/acp-8-1343-2008, 2008.

15 Nordmann, S., Birmili, W., Weinhold, K., Müller, K., Spindler, G., and Wiedensohler, A.:
16 Measurements of the mass absorption cross section of atmospheric soot particles using Raman
17 spectroscopy, *J. Geophys. Res.-Atmos.*, 118, 12075–12085, doi:10.1002/2013JD020021,
18 2013.

19 Nordmann, S., Cheng, Y. F., Carmichael, G. R., Yu, M., Denier van der Gon, H. A. C., Zhang,
20 Q., Saide, P. E., Pöschl, U., Su, H., Birmili, W., and Wiedensohler, A.: Atmospheric black
21 carbon and warming effects influenced by the source and absorption enhancement in central
22 Europe, *Atmos. Chem. Phys.*, 14, 12683–12699, doi:10.5194/acp-14-12683-2014, 2014.

23 Petzold, A. and Kärcher, B.: Aerosols in the Atmosphere, in: *Atmospheric Physics*, edited by:
24 Schumann, U., *Research Topics in Aerospace*, Springer Berlin Heidelberg, 37–53,
25 doi:10.1007/978-3-642-30183-4_3, 2012.

26 Pouliot, G., Pierce, T., van der Gon, H., Schaap, M., Moran, M., and Nopmongcol, U.:
27 Comparing emission inventories and model-ready emission datasets between Europe and
28 North America for the AQMEII project, *Atmos. Environ.*, 53, 4–14, 2012.

29 Pope, C. A., Ezzati, M., and Dockery, D. W.: Fine-particulate air pollution and life expectancy
30 in the united states, *N. Engl. J. Med.*, 360, 376–386, 2009.

31 Poulain, L., Spindler, G., Birmili, W., Plass-Dülmer, C., Wiedensohler, A., and Herrmann, H.:

1 Seasonal and diurnal variations of particulate nitrate and organic matter at the IfT research
2 station Melpitz, *Atmos. Chem. Phys.*, 11, 12579–12599, doi:10.5194/acp-11-12579-2011,
3 2011.

4 Ramanathan, V. and Carmichael, G.: Global and regional climate changes due to black
5 carbon, *Nat. Geosci.*, 1, 221–227, 2008.

6 Rose, D., Wehner, B., Ketzler, M., Engler, C., Voigtländer, J., Tuch, T., and Wiedensohler, A.:
7 Atmospheric number size distributions of soot particles and estimation of emission factors,
8 *Atmos. Chem. Phys.*, 6, 1021–1031, doi:10.5194/acp-6-1021-2006, 2006.

9 Saide, P. E., Spak, S. N., Carmichael, G. R., Mena-Carrasco, M. A., Yang, Q., Howell, S.,
10 Leon, D. C., Snider, J. R., Bandy, A. R., Collett, J. L., Benedict, K. B., de Szoeke, S. P.,
11 Hawkins, L. N., Allen, G., Crawford, I., Crosier, J., and Springston, S. R.: Evaluating
12 WRFChem aerosol indirect effects in Southeast Pacific marine stratocumulus during
13 VOCALSREx, *Atmos. Chem. Phys.*, 12, 3045–3064, doi:10.5194/acp-12-3045-2012, 2012.

14 Spindler, G., Brüggemann E., Gnauk, T., Grüner A., Müller K., and Herrmann, H.: A four-
15 year size-segregated characterization study of particles PM₁₀, PM_{2.5} and PM₁ depending on
16 air mass origin at Melpitz, *Atmos. Environ.*, 44, 164–173, 2010.

17 Spindler, G., Gnauk, T., Grüner, A., Iinuma, Y., Müller, K., Scheinhardt, S., and Herrmann,
18 H.: Size-segregated characterization of PM₁₀ at the EMEP site Melpitz (Germany) using a
19 fivestage impactor: a 6 year study, *J. Atmos. Chem.*, 69, 127–157, 2012.

20 Spindler, G., Grüner, A., Müller, K., Schlimper, S., and Herrmann, H.: Long-term
21 sizesegregated particle (PM₁₀, PM_{2.5}, PM₁) characterization study at Melpitz – influence of
22 air mass inflow, weather conditions and season, *J. Atmos. Chem.*, 70, 165–195,
23 doi:10.1007/s10874-013-9263-8, 2013.

24 Stern, R., Builtjes, P., Schaap, M., Timmermans, R., Vautard, R., Hodzic, A., Memmesheimer,
25 M., Feldmann, H., Renner, E., Wolke, R., and Kerschbaumer: a model inter-comparison study
26 focussing on episodes with elevated PM₁₀ concentrations, *Atmos. Environ.*, 42, 4567–4588,
27 doi:10.1016/j.atmosenv.2008.01.068, 2008.

28 Vignati, E., Karl, M., Krol, M., Wilson, J., Stier, P., and Cavalli, F.: Sources of uncertainties in
29 modelling black carbon at the global scale, *Atmos. Chem. Phys.*, 10, 2595–2611,
30 doi:10.5194/acp-10-2595-2010, 2010.

31 Visschedijk, A. and Denier van der Gon, H.: EUCAARI Deliverable: Pan-European

- 1 Carbonaceous Aerosol Inventory, Report, TNO Built Environment and Geosciences, D42,
2 Utrecht, the Netherlands, 2008.
- 3 Wiedinmyer, C., Akagi, S. K., Yokelson, R. J., Emmons, L. K., Al-Saadi, J. A., Orlando, J. J.,
4 and Soja, A. J.: The Fire INventory from NCAR (FINN): a high resolution global model to
5 estimate the emissions from open burning, *Geosci. Model Dev.*, 4, 625–641,
6 doi:10.5194/gmd-4-625-2011, 2011.
- 7 Wild, O., Zhu, X., and Prather, M. J.: Fast-J: accurate simulation of in- and below-cloud
8 photolysis in tropospheric chemical models, *J. Atmos. Chem.*, 37, 245–282, 2000.
- 9 Zhang, Y., Sartelet, K., Zhu, S., Wang, W., Wu, S.-Y., Zhang, X., Wang, K., Tran, P., Seigneur,
10 C., and Wang, Z.-F.: Application of WRF/Chem-MADRID and WRF/Polyphemus in Europe –
11 Part 2: Evaluation of chemical concentrations and sensitivity simulations, *Atmos. Chem.*
12 *Phys.*, 13, 6845–6875, doi:10.5194/acp-13-6845-2013, 2013.
- 13 Zaveri, R. A. and Peters, L. K.: A new lumped structure photochemical mechanism for
14 largescale applications, *J. Geophys. Res.*, 104, 30387–30415, 1999.
- 15 Zaveri, R. A., Easter, R. C., Fast, J. D., and Peters, L. K.: Model for Simulating Aerosol
16 Interactions and Chemistry (MOSAIC), *J. Geophys. Res.*, 113, D13204,
17 doi:10.1029/2007JD008782, 2008.

18

Table 1. Sectional approach for aerosols: Particle dry-diameter ranges used in this study.

	Bin 01	Bin 02	Bin 03	Bin 04	Bin 05	Bin 06	Bin 07	Bin 08
Minimum Diameter (μm)	0.0390625	0.078125	0.15625	0.3125	0.625	1.25	2.5	5.0
Maximum Diameter (μm)	0.078125	0.15625	0.3125	0.625	1.25	2.5	5.0	10.0

1

Table 2. Configurations of WRF-Chem

Physics	WRF option
Micro physics	Lin et. al., 1983 scheme
Surface	Rapid Update Cycle (RUC) land surface model
Boundary layer	YSU (Hong et. al., 2006)
Cumulus	Grell 3D
Urban	3-category UCM
Shortwave radiation	Goddard shortwave (Chou et. al., 1998)
Longwave radiation	New Goddard scheme
Chemistry and Aerosol	Chem option
Gas-phase mechanism	CBMZ
Aerosol module	MOSAIC with 8 bins
Photolytic rate	Fast-J photolysis scheme

1

1 **Table 3.** Comparison result for meteorological variables between Melpitz radio-sounding
2 measurements and WRF-Chem model

	Slope	R²	Data point Number
Potential Temperature	0.99	0.98	586
Water Vapor Mixing Ratio	0.81	0.84	586
Wind Speed	0.90	0.93	586
Wind Direction	1.02	0.70	586

3

1 **Table 4.** Comparison between the adjusted EC coarse emission simulation and original one

Sites	Adjusted EC coarse fraction			Original (Nordmann et. al., 2014)			Air mass
	MB	MNB	R²	MB	MNB	R²	
Bösel	0.12	0.13	0.81	-0.31	-0.21	0.61	East
Leipzig-TROPOS	-1.01	-0.47	0.69	-1.57	-0.7	0.35	East
Hohenpeißenberg	-0.52	-0.64	0.43	-0.59	-0.72	0.66	Southeast
Zugspitze	-0.22	-0.56	0.72	-0.26	-0.46	0.79	Southeast

2

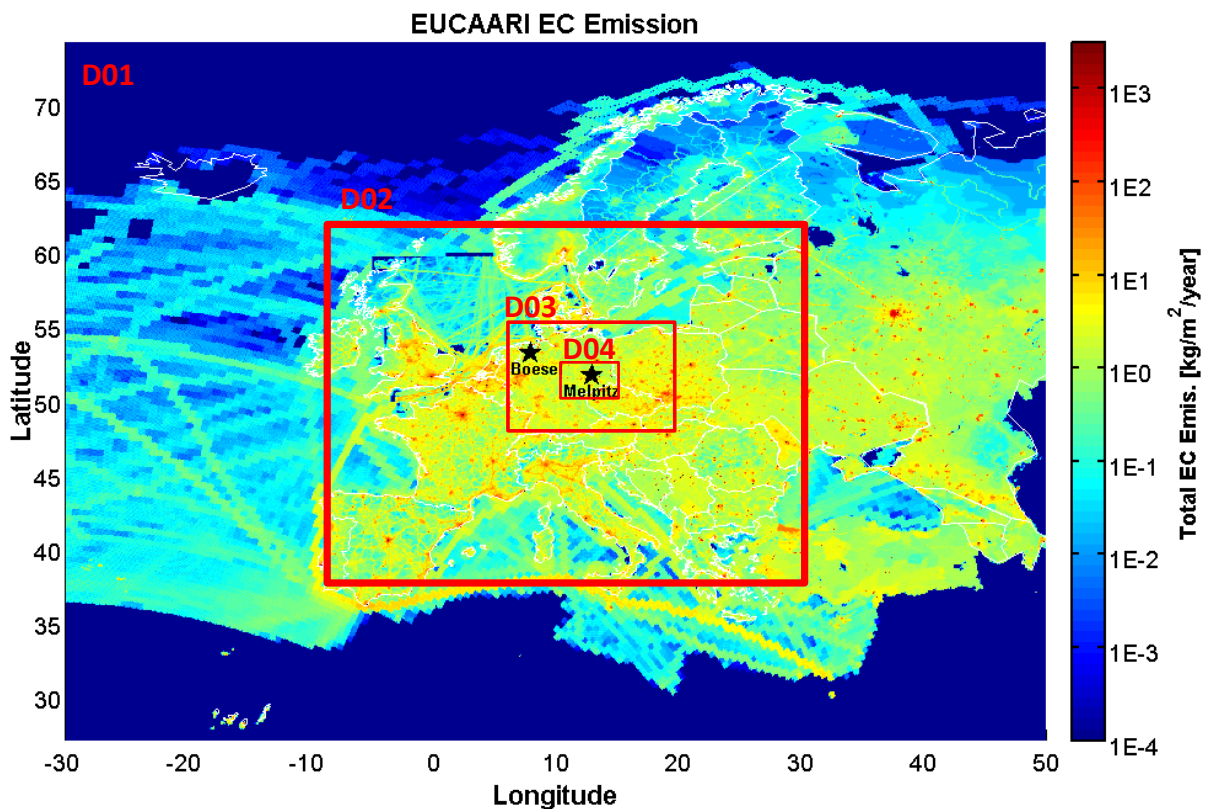


Figure 1. EUCARRI (resolution 7 km) EC emission ($\text{kg m}^{-2} \text{ year}^{-1}$). The 4 nested model domains (D01-D04) are indicated in the picture. Melpitz and Bösel (Boesel) are marked by black stars.

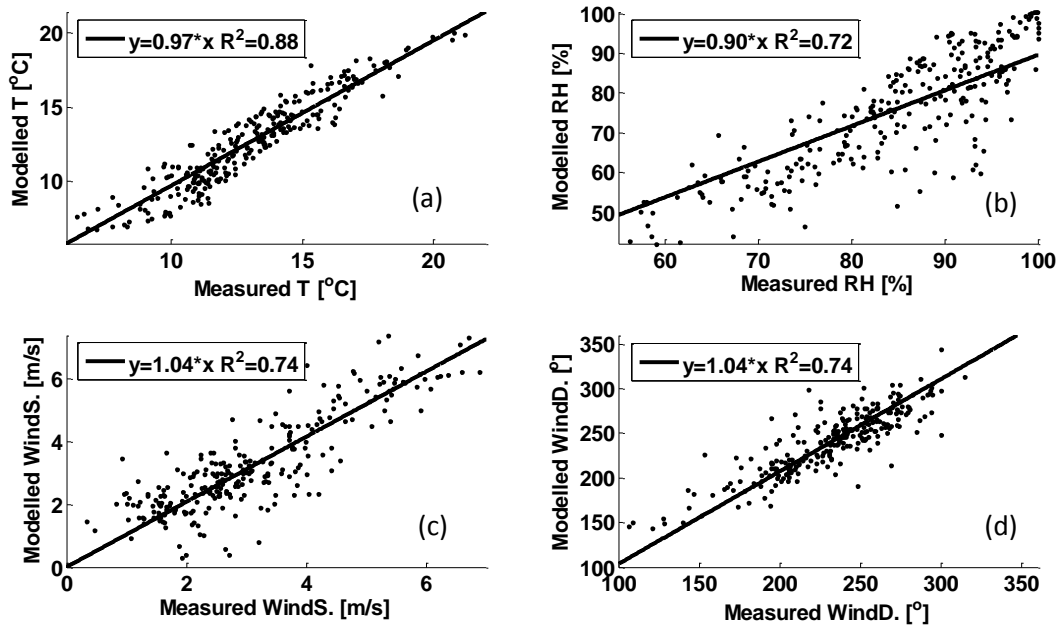


Figure 2. Comparison of meteorological variables between Melpitz ground-based measurements and WRF-Chem D04 result. (a) Temperature; (b) Relative Humidity; (C) Wind Speed; (D) Wind Direction.

1

2

1

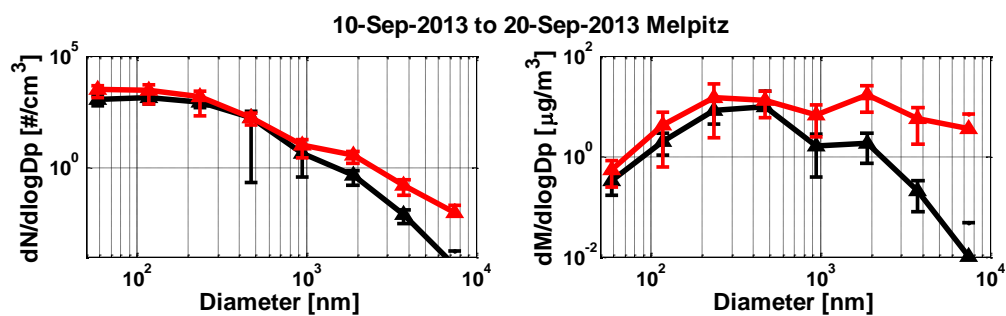


Figure 3. Comparison of Particle Number Size Distribution (PNSD, left) and Particle Mass Size Distribution (PMSD, right) between WRF-Chem model and Melpitz measurements. Model results indicated by the red lines and measurements by the black lines. The size distributions are averaged in the period 10-20 September 2013, the error bar indicate the upper and lower limits.

2

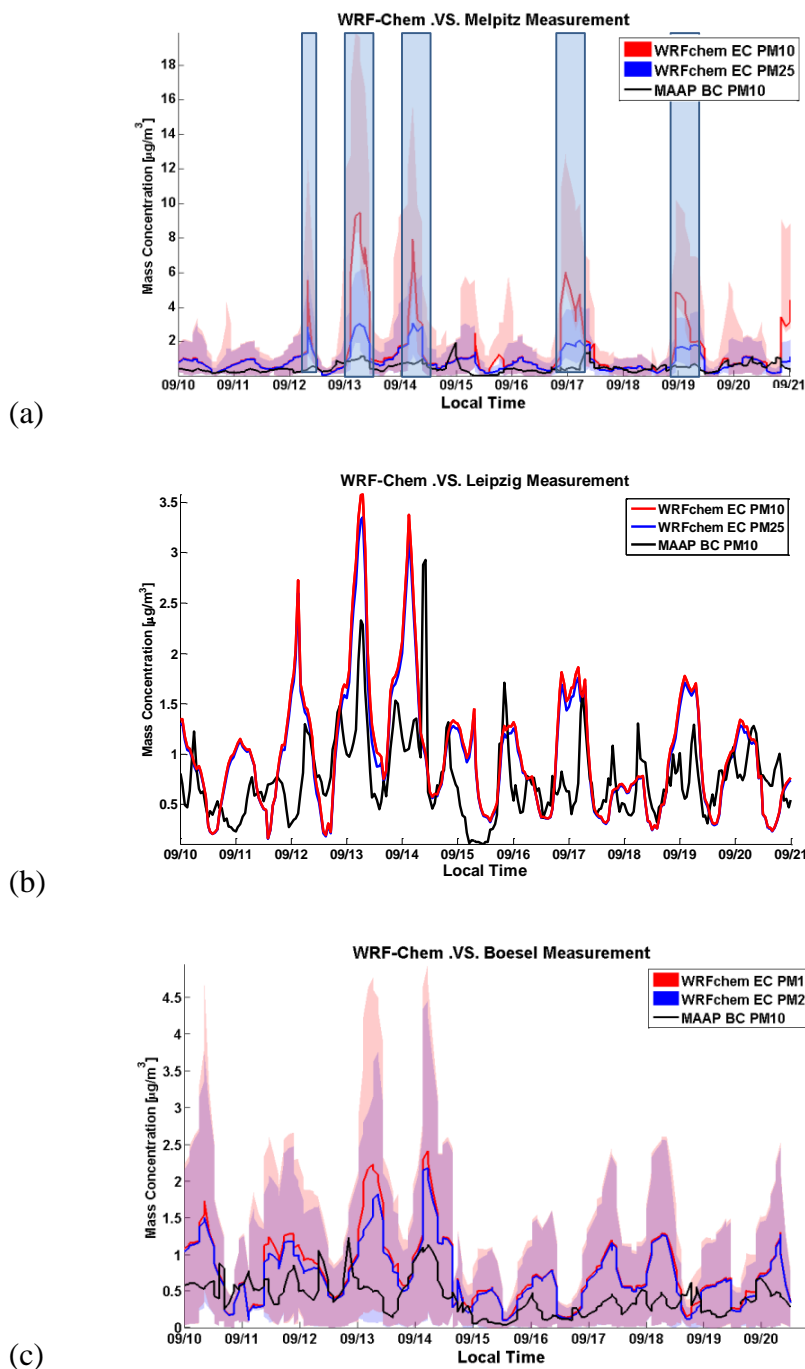


Figure 4. The comparison of EC/BC concentration between model and MAAP measurements. Red line: EC concentration in PM10 of model result; blue line: EC concentration in PM2.5 of model result; black line: BC concentration in PM10 of MAAP measurement, used as the best approximation of EC. The shaded areas indicate the model uncertainty defined by the maxima (upper limit of the shade) and minima (lower limit of the shade) values within 12 km distance from Melpitz / Bösel. The blue rectangles mark the EC plume episodes at Melpitz. (a) Melpitz: modelling result derived from D04 simulation with 2km resolution; (b) Leipzig-TROPOS: modelling result derived from D04 simulation with 2km resolution; (c) Bösel: modelling result derived from D03 simulation with 6km resolution.

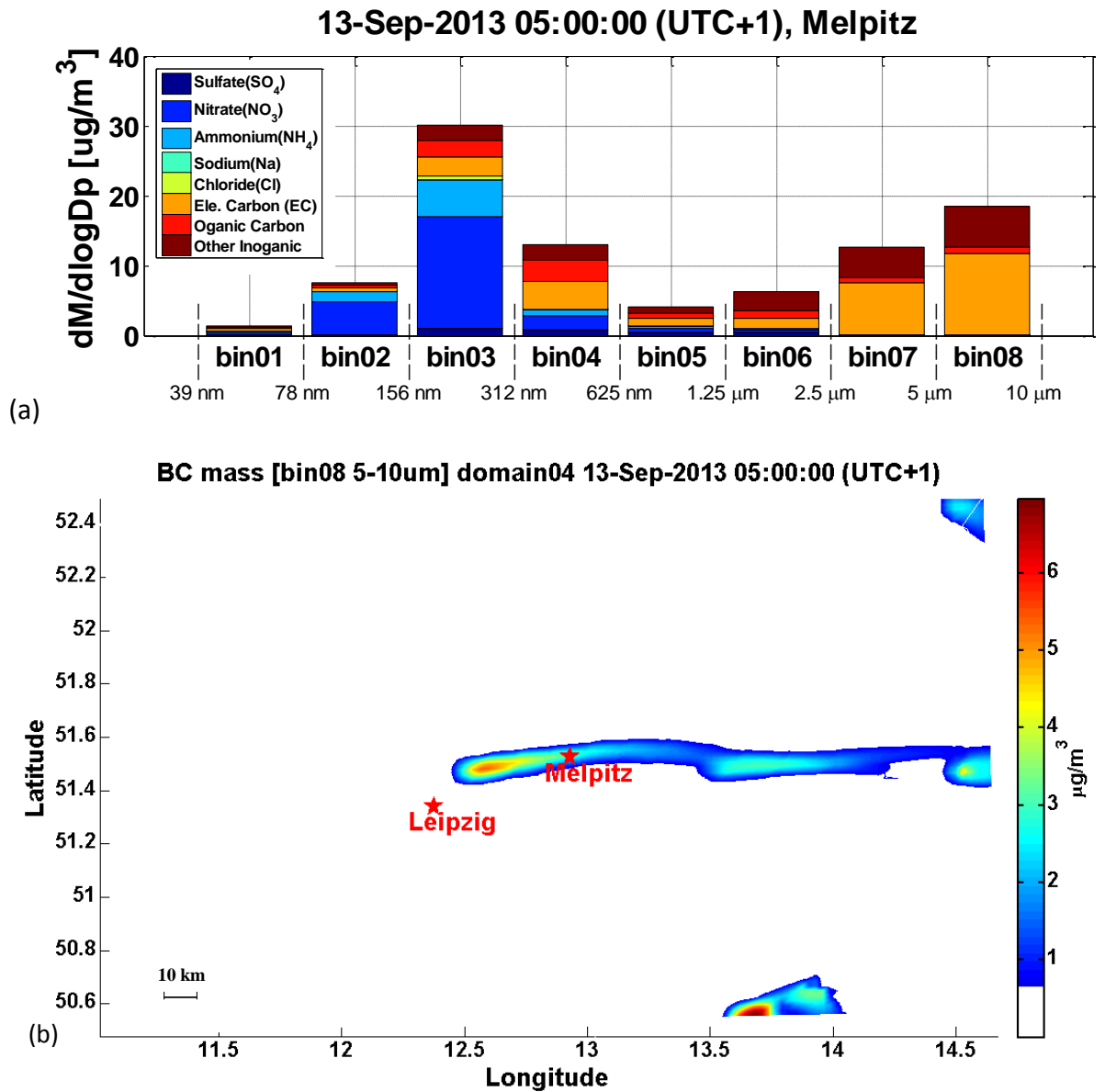


Figure 5. The model result: (a) aerosol chemistry compounds for each bins of Melpitz; (b) horizontal distribution of EC in bin08 [5-10 μm] at 05:00 (UTC+1) of 13 September 2013

1

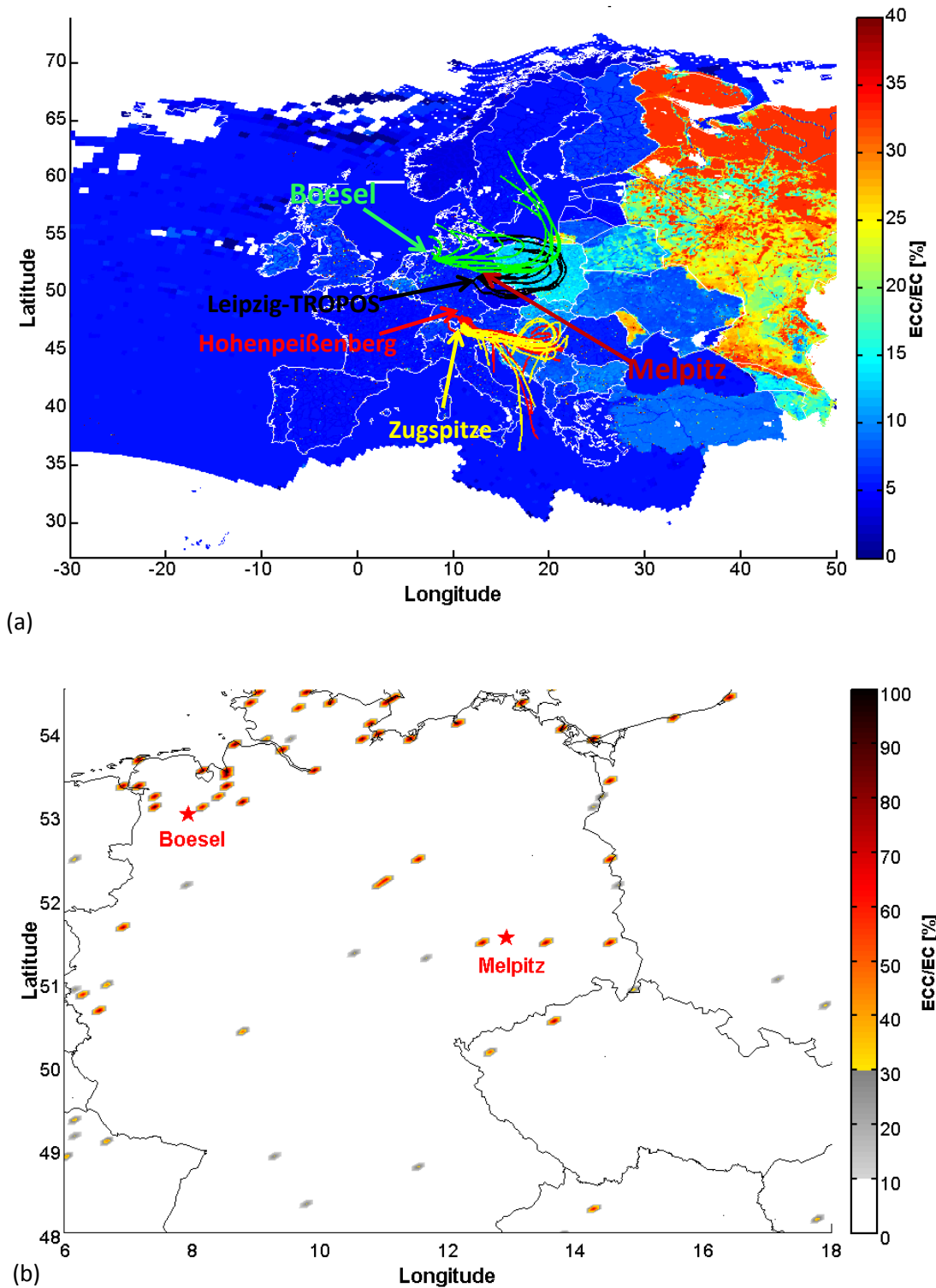


Figure 6. EUCAARI EC emission coarse mode fraction (ECc). (a) ECc result of total emission, including area and point sources. The location of B ösel, Leipzig-TROPOS, Melpitz, Hohenpeissenberg and Zugspitze are marked in the map. The colored lines indicated the 3-days back trajectories for each site (without Melpitz), in the period from 2009-04-01 to 2009-04-04 with 6 hours interval. (b) ECc result of point source emissions.

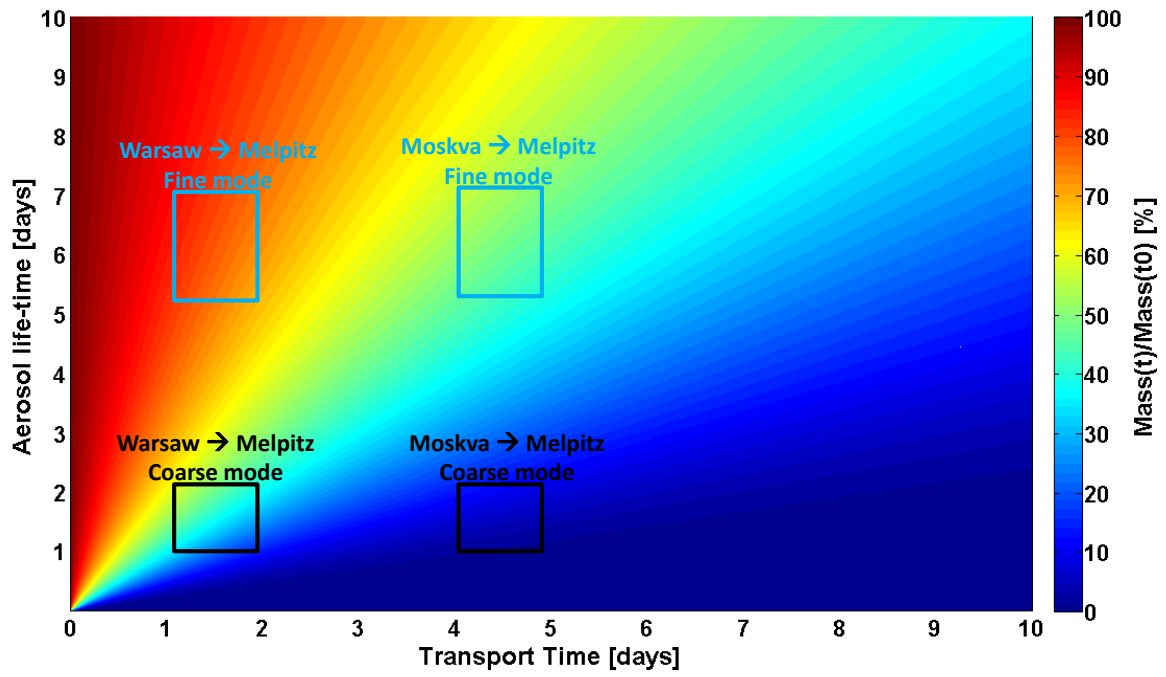


Figure 7. Aerosol mass residential rate with relationship of transport time and lifetime. The color indicates the percentage of aerosol mass that can be transported to Melpitz.

1